Electroexcitation of the $\Delta^+(1232)$ at low momentum transfer

A. Blomberg [a], D. Anez [b,c], N. Sparveris [a,*], A.J. Sarty [c], M. Paolone [a], S. Gilad [d], D. Higinbotham [e], Z. Ahmed [f], H. Albataineh [g], K. Allada [e], B. Anderson [h], K. Aniol [i], J. Annand [j], J. Arrington [k], T. Averett [l], H. Baghdasaryan [m], X. Bai [n], A. Beck [o], S. Beck [o], V. Bellini [p], F. Benmokhtar [q], W. Boeglin [r], C.M. Camacho [s], A. Camsonne [e], C. Chen [t], J.P. Chen [e], K. Chirapatpimol [m,u], E. Cisbani [v], M. Dalton [m], W. Deconinck [l], M. Defurne [w], R. De Leo [x], D. Flay [a], N. Fomin [y], M. Friend [z], S. Frullani [v,aa], E. Fuchey [a], F. Garibaldi [v], R. Gilman [ab], C. Gu [m], D. Hamilton [j], C. Hanretty [m,ac], O. Hansen [e], M. Hashemi Shabestari [m], O. Hen [ad], T. Holmstrom [ae], M. Huang [af], S. Iqbal [i], N. Kalantarians [ag], H. Kang [ah], A. Kelleher [ai], M. Khandaker [aj], I. Korover [ad], J. Leckey [aj], J. LeRose [e], R. Lindgren [m], E. Long [h], J. Mammei [ak], D.J. Margaziotis [i], A. Martí Jimenez-Arguello [al], D. Meekins [e], Z.E. Meziani [a], M. Mihovilovic [am], N. Muangma [ai], B. Norum [m], Nuruzzaman [an], K. Pan [d], S. Phillips [ao], E. Piasetzky [ad], A. Polychronopoulou [a], I. Pomerantz [ad], M. Posik [a], V. Punjabi [ap], X. Qian [af], A. Rakhman [aq], P.E. Reimer [k], S. Riordan [ar,as], G. Ron [at], A. Saha [e], E. Schulte [a], L. Selvy [h], R. Shneor [ad], S. Sirca [au], J. Sjoegren [j], R. Subedi [av], V. Sulkosky [e], W. Tireman [aw], D. Wang [m], J. Watson [h], B. Wojtsekhowski [e], W. Yan [ax], I. Yaron [ad], Z. Ye [m], X. Zhan [k], J. Zhang [e], Y. Zhang [ab], B. Zhao [ay], Z. Zhao [m], X. Zheng [m], P. Zhu [ax]

[a] Temple University, Philadelphia, PA 19122, USA
[b] Dalhousie University, Halifax, Nova Scotia, Canada
[c] Saint Mary's University, Halifax, Nova Scotia, Canada
[d] Massachusetts Institute of Technology, Cambridge, MA 02139, USA
[e] Thomas Jefferson National Accelerator Facility, Newport News, VA 23606, USA
[f] Syracuse University, Syracuse, NY 13210, USA
[g] Old Dominion University, Norfolk, VA 23529, USA
[h] Kent State University, Kent, OH 44242, USA
[i] California State University, Los Angeles, Los Angeles, CA 90032, USA
[j] University of Glasgow, Glasgow G12 8QQ, Scotland, UK
[k] Physics Division, Argonne National Laboratory, Argonne, IL 60439, USA
[l] The College of William and Mary, Williamsburg, VA 23187, USA
[m] University of Virginia, Charlottesville, VA 22904, USA
[n] China Institute of Atomic Energy, Beijing, China
[o] Nuclear Research Center-Negev, Beer-Sheva, Israel
[p] Universita di Catania, Catania, Italy
[q] Duquesne University, Pittsburgh, PA 15282, USA
[r] Florida International University, Miami, FL 33199, USA
[s] Institut de Physique Nucleaire, Orsay, France
[t] Hampton University, Hampton, VA 23668, USA
[u] Chiang Mai University, Chiang Mai, Thailand
[v] INFN, Sezione di Roma, I-00161 Rome, Italy
[w] École Centrale Paris, Châtenay-Malabry, France
[x] Universite di Bari, Bari, Italy
[y] University of Tennessee, Knoxville, TN 37996, USA
[z] Carnegie Mellon University, Pittsburgh, PA 15213, USA
[aa] Istituto Superiore di Sanità, I-00161 Rome, Italy
[ab] Rutgers University, New Brunswick, NJ 08855, USA
[ac] Florida State University, Tallahassee, FL 32306, USA
[ad] Tel Aviv University, Tel Aviv 69978, Israel

* Corresponding author.
  E-mail address: sparveri@temple.edu (N. Sparveris).

[ae] *Longwood University, Farmville, VA 23909, USA*
[af] *Duke University, Durham, NC 27708, USA*
[ag] *Unversity of Houston, Houston, TX 77030, USA*
[ah] *Seoul National University, Seoul, Republic of Korea*
[ai] *MIT Bates Linear Accelerator, Middleton, MA 01949, USA*
[aj] *Indiana University, Bloomington, IN 47405, USA*
[ak] *Virginia Polytechnic Institute and State University, Blacksburg, VA 24061, USA*
[al] *Laboratoire de Physique Corpusculaire de Clermont-Ferrand, Aubière Cedex, France*
[am] *Jožef Stefan Institute, Ljubljana, Slovenia*
[an] *Mississippi State University, Mississippi State, MS 39762, USA*
[ao] *University of New Hampshire, Durham, NH 03824, USA*
[ap] *Norfolk State University, Norfolk, VA 23504, USA*
[aq] *Spallation Neutron Source, Oak Ridge National Laboratory, Oak Ridge, TN 37831, USA*
[ar] *University of Massachusetts, Amherst, MA 01003, USA*
[as] *Stony Brook University, Stony Brook, NY 11794, USA*
[at] *Racah Institute of Physics, Hebrew University of Jerusalem, Jerusalem, 91904, Israel*
[au] *University of Ljubljana, Ljubljana, Slovenia*
[av] *George Washington University, Washington, DC 20052, USA*
[aw] *Northern Michigan University, Marquette, MI 49855, USA*
[ax] *University of Science and Technology of China, Hefei 230026, People's Republic of China*
[ay] *University of Connecticut, Storrs, CT 06269, USA*

A R T I C L E   I N F O

A B S T R A C T

We report on new p($e, e'p$)π° measurements at the $\Delta^+(1232)$ resonance at the low momentum transfer region, where the mesonic cloud dynamics is predicted to be dominant and rapidly changing, offering a test bed for chiral effective field theory calculations. The new data explore the Q^2 dependence of the resonant quadrupole amplitudes and for the first time indicate that the Electric and the Coulomb quadrupole amplitudes converge as $Q^2 \rightarrow 0$. The measurements of the Coulomb quadrupole amplitude have been extended to the lowest momentum transfer ever reached, and suggest that more than half of its magnitude is attributed to the mesonic cloud in this region. The new data disagree with predictions of constituent quark models and are in reasonable agreement with dynamical calculations that include pion cloud effects, chiral effective field theory and lattice calculations. The measurements indicate that improvement is required to the theoretical calculations and provide valuable input that will allow their refinements.

The $\Delta(1232)$ resonance – the first excited state of the nucleon – dominates many nuclear phenomena at energies above the pion-production threshold and plays a prominent role in the physics of the strong interaction. The study of the Δ has allowed to explore various aspects of the nucleonic structure, such as the study of d-wave components that could quantify to what extent the nucleon or the Δ wave function deviates from the spherical shape [1], or more recently the exploration of the Generalized Polarizabilities (GPs) of the nucleon which, contrary to the elastic form factors, are sensitive to all the excited spectrum of the nucleon [3,2,4].

Hadrons are composite systems with complex quark–gluon and meson cloud dynamics that give rise to non-spherical components in their wavefunction, which in a classical limit and at large wavelengths will correspond to a "deformation" [6,7,5]. The determination and subsequent understanding of the shapes of the fundamental building blocks in nature is a particularly fertile line of investigation for the understanding of the interactions of their constituents amongst themselves and the surrounding medium. For hadrons this means the interquark interaction and the quark–gluon dynamics. For the proton, the only stable hadron, the vanishing of the spectroscopic quadrupole moment, due to its spin 1/2 nature, precludes access to the most direct observable of deformation. As a result, the presence of the resonant quadrupole amplitudes $E_{1+}^{3/2}$ and $S_{1+}^{3/2}$ (or E2 and C2 photon absorption multipoles respectively) in the predominantly magnetic dipole $M_{1+}^{3/2}$ (or M1) $\gamma^* N \rightarrow \Delta$ transition has emerged as the experimental signature for such an effect [1,5–51]. Nonvanishing quadrupole amplitudes will signify

that either the proton or the $\Delta^+(1232)$ or more likely both are characterized by non-spherical components in their wavefunctions. These amplitudes have been explored up to four momentum transfer squared $Q^2 = 7$ (GeV/c)² [10–26,37–43]. Their relative strength is normally quoted in terms of the ratios EMR $= Re(E_{1+}^{3/2}/M_{1+}^{3/2})$ and CMR $= Re(S_{1+}^{3/2}/M_{1+}^{3/2})$. The experimental results are in reasonable agreement with models invoking the presence of non-spherical components in the nucleon wavefunction.

In the constituent-quark picture of hadrons, the non-spherical amplitudes are a consequence of the non-central, color-hyperfine interaction among quarks [7,8]. However, it has been shown that this mechanism only provides a small fraction of the observed quadrupole signal at low momentum transfers, with the magnitudes of this effect for the predicted E2 and C2 amplitudes [9] being at least an order of magnitude too small to explain the experimental results and with the dominant M1 matrix element being $\approx 30\%$ low. A likely cause of these dynamical shortcomings is that such quark models do not respect chiral symmetry, whose spontaneous breaking leads to strong emission of virtual pions (Nambu–Goldstone Bosons) [1]. These couple to nucleons as $\vec{\sigma} \cdot \vec{p}$ where $\vec{\sigma}$ is the nucleon spin, and $\vec{p}$ is the pion momentum. The coupling is strong in the p wave and mixes in non-zero angular momentum components. Based on this, it is physically reasonable to expect that the pionic contributions increase the M1 and dominate the E2 and C2 transition matrix elements in the low Q^2 (large distance) domain. This was first indicated by adding pionic effects to quark models [45–47], subsequently in pion cloud model calcu-

lations [31,32], and recently demonstrated in Chiral Effective Field Theory calculations [48]. With the existence of these non-spherical amplitudes well established recent high precision experiments and theoretical efforts have focused on testing in depth the reaction calculations and decoding the underlying nucleon dynamics.

More recently the study of the $N \to \Delta$ transition has emerged as an excellent testing ground to study the Generalized Polarizabilities of the nucleon [3,2,4]. The GPs are fundamental quantities of the nucleon. They can be seen as Fourier transforms of local polarization densities (electric, magnetic, and spin) allowing us to study the role of the pion cloud and quark core contributions at various length scales. The sensitivity to the GPs grows significantly in the resonance region, and the precise knowledge of the $N \to \Delta$ transition form factors is required as an input to Dispersions Relations calculations [52,53] in order to extract the GPs from Virtual Compton Scattering measurements at the resonance region.

In this Letter we report on π° reaction channel measurements at the low momentum transfer region. The new data explore the Q^2 dependence of the quadrupole amplitudes with high precision, and extend the measurements of the Coulomb quadrupole amplitude to a new lowest momentum transfer. The cross section of the $p(\vec{e}, e'p)\pi^\circ$ reaction is sensitive to five independent partial responses ($\sigma_T, \sigma_L, \sigma_{LT}, \sigma_{TT}$ and $\sigma_{LT'}$) [35]:

$$\frac{d^5\sigma}{d\omega d\Omega_e d\Omega_{pq}^{cm}} = \Gamma(\sigma_T + \epsilon \cdot \sigma_L - v_{LT} \cdot \sigma_{LT} \cdot \cos \phi_{pq}^*$$
$$+ \epsilon \cdot \sigma_{TT} \cdot \cos 2\phi_{pq}^* \qquad (1)$$
$$- h \cdot p_e \cdot v_{LT'} \cdot \sigma_{LT'} \cdot \sin \phi_{pq}^*)$$

where $v_{LT} = \sqrt{2\epsilon(1+\epsilon)}$ and $v_{LT'} = \sqrt{2\epsilon(1-\epsilon)}$ are kinematic factors, ϵ is the transverse polarization of the virtual photon, Γ is the virtual photon flux, $h = \pm 1$ is the electron helicity, p_e is the magnitude of the electron longitudinal polarization, and ϕ_{pq}^* is the proton azimuthal angle with respect to the electron scattering plane. The differential cross sections ($\sigma_T, \sigma_L, \sigma_{LT}, \sigma_{TT}$, and $\sigma_{LT'}$) are all functions of the center-of-mass energy W, the Q^2, and the proton center of mass polar angle θ_{pq}^* (measured from the momentum transfer direction) [35]. The $\sigma_0 = \sigma_T + \epsilon \cdot \sigma_L$ response is dominated by the M_{1+} resonant multipole while the interference of the $C2$ and $E2$ amplitudes with the $M1$ dominates the Longitudinal–Transverse and Transverse–Transverse responses, respectively.

Measurements were made in Hall A at Jefferson Lab. A 15 μA to 80 μA, 1160 MeV electron beam impinged on a 4 cm liquid–hydrogen target. Electrons and protons were detected in coincidence with the two High Resolution Spectrometers (HRS) [54]. Both spectrometers employ a pair of vertical drift chambers for track reconstruction, three scintillator panels for trigger, timing, and detector efficiencies, as well as two layers of lead glass calorimeters. The electron spectrometer utilized a gas Cherenkov detector. Both spectrometers are characterized by a momentum resolution of 10^{-4} and a spectrometer angle determination accuracy of 0.1 mr.

Measurements were performed from $Q^2 = 0.04$ to $Q^2 = 0.13$ (GeV/c)^2. For each θ_{pq}^* setting the proton spectrometer was sequentially placed at $\phi_{pq}^* = 0°$ and $180°$, thus allowing to extract the σ_{LT} and the $\sigma_0 + \epsilon \cdot \sigma_{TT}$ responses. The in-plane azimuthal asymmetry of the cross section with respect to the momentum transfer direction, $A_{(\phi_{pq}=0,\pi)} = [\sigma_{\phi_{pq}=0} - \sigma_{\phi_{pq}=180}]/[\sigma_{\phi_{pq}=0} + \sigma_{\phi_{pq}=180}]$, which exhibits sensitivity to the Coulomb quadrupole amplitude, was also determined. Measurements of the parallel cross section σ_0 were also performed in the range of W = 1170 MeV to 1232 MeV. A first level of acceptance cuts was applied in the data analysis in order to limit the phase space to the central region of the spectrometers and to ensure that potential edge effects will be avoided. For the pair of $\phi_{pq}^* = 0°$ and

180° measurements the cross sections, responses, and asymmetries were obtained with the phase space matched in (W, Q^2, θ_{pq}^*). Point cross sections were extracted from the finite acceptances by utilizing the cross section calculations from various theoretical models [32–36] in the Monte Carlo simulation. Radiative corrections were applied to the data using a Monte Carlo simulation [55]. The cross section systematic uncertainties are of the order of $\pm 3\%$, dominating over the better than $\pm 1\%$ statistical uncertainties. In the asymmetry measurements the systematic uncertainties were further suppressed through the cross section ratio, while an advantage is presented by the fact that the electron spectrometer position and momentum settings do not change during the asymmetry measurements. A detailed description of the data analysis is presented in [56,57].

In Fig. 1 the experimental results for σ_{LT} and $\sigma_0 + \epsilon \cdot \sigma_{TT}$ are presented, and in Fig. 2 the asymmetry measurements are exhibited. In Fig. 2 the measurement of the parallel cross section σ_o at $Q^2 = 0.13$ (GeV/c)^2 as a function of W is also presented. The experimental results are compared with the SAID multipole analysis [36], the phenomenological model MAID 2007 [34,33] and the dynamical model calculations of Sato–Lee [31] and of Dubna–Mainz–Taipei (DMT) [32]. The Sato–Lee [31] and DMT [32] are dynamical reaction models which include pionic cloud effects. Both calculate the resonant channels from dynamical equations. DMT uses the background amplitudes of MAID with some small modifications. Sato–Lee calculate all amplitudes consistently within the same framework with only three free parameters. Both find that a large fraction of the quadrupole multipole strength arises due to the pionic cloud with the effect reaching a maximum value in this momentum transfer region. Sato–Lee exhibits a relatively good agreement with the σ_{LT} measurements as one moves to lower Q^2 while DMT systematically overestimates this response indicating an overestimation of the Coulomb quadrupole amplitude. Both calculations provide a reasonable agreement to the σ_o measurements as a function of W as shown in Fig. 2. On the other hand the MAID model [33,34] which offers a flexible phenomenology, as well as the SAID multipole analysis, fail to reproduce the W-dependence of the σ_o measurements. This observation is in agreement with previous measurements [39,43] that suggest that both calculations need to be refined, especially at the lower wing of the resonance. Both calculations perform reasonably well at the higher Q^2 measurements but their predictions deviate more as one moves lower in Q^2, as indicated by Fig. 1 and Fig. 2.

Fits of the resonant amplitudes have been performed while taking into account the contributions of background amplitudes from the MAID, DMT, SAID, and Sato–Lee models. The fitting procedure is described in detail in [57] and it is the same that has been applied before in various experiments [38,39,43]. The resonant amplitudes are fitted while utilizing the background amplitudes from each theoretical model calculation separately. The models differ in their description of the background terms thus leading to a deviation of the fitted results which indicates the level of the model uncertainty. The deviation of the fitted central values is adopted as a model uncertainty of the extracted amplitudes. For the CMR ratio, at $Q^2 = 0.13$ (GeV/c)^2 we find a value of $(-4.80 \pm 0.19_{stat+sys} \pm 0.80_{model})\%$ which is in excellent agreement with the recent MAMI measurement [43]. For $Q^2 = 0.09$ (GeV/c)^2 and $Q^2 = 0.04$ (GeV/c)^2 we find that the CMR is $(-3.50 \pm 0.20_{stat+sys} \pm 0.80_{model})\%$ and $(-3.00 \pm 0.27_{stat+sys} \pm 0.80_{model})\%$ respectively. The EMR results, $(-2.50 \pm 0.50_{stat+sys} \pm 0.50_{model})\%$ at $Q^2 = 0.13$ (GeV/c)^2 and $(-1.90 \pm 0.50_{stat+sys} \pm 0.50_{model})\%$ at $Q^2 = 0.09$ (GeV/c)^2, confirm earlier measurements [39] that indicate that the ratio stays within 2%–2.5% in this region. The derived CMR values are presented in Fig. 3. One can observe a disagree-
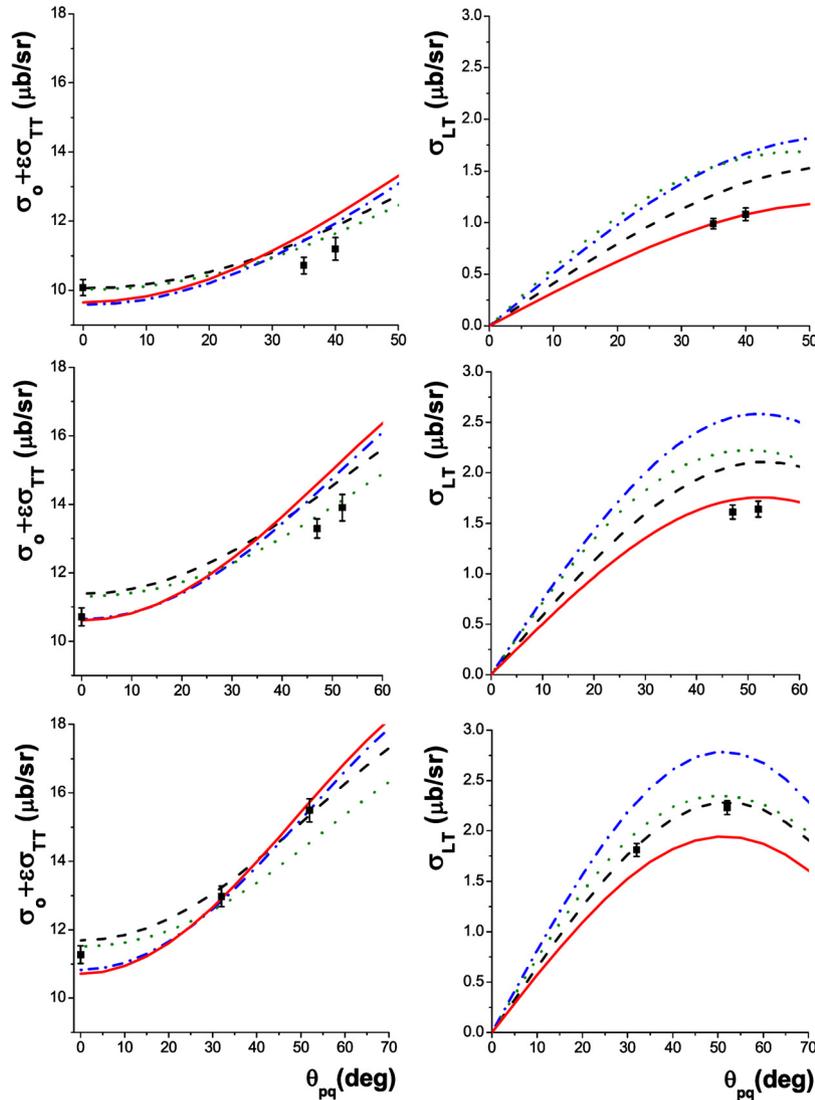
Fig. 1. Measurements of $\sigma_0 + \epsilon \cdot \sigma_{TT}$ and σ_{LT} at $Q^2 = 0.04$ (GeV/c)^2 (top panels), $Q^2 = 0.09$ (GeV/c)^2 (center), and $Q^2 = 0.13$ (GeV/c)^2 (bottom). The theoretical predictions of DMT [32] (dash-dot), SAID [36] (dot), MAID [33,34] (dash), and Sato–Lee [31] (solid) are also presented.

ment between the MAMI result at $Q^2 = 0.06$ (GeV/c)^2 [25] and the new data. The source of this disagreement has been identified in the extraction procedure [25] of the resonant amplitudes from the measured MAMI cross sections. A revised extraction procedure corrects the CMR value at $Q^2 = 0.06$ (GeV/c)^2 [25], moving it towards the new data by approximately 1% thus reconciling this discrepancy; details of this revised work will be presented in an upcoming publication.

As exhibited in Fig. 3 the Sato–Lee prediction has a remarkable success in describing the Q^2 evolution of the Coulomb quadrupole amplitude. The DMT, MAID, and SAID calculations are less effective and tend to overestimate the magnitude of the ratio. The data provide a strong support to the interpretation within the Sato–Lee model that the Δ resonance consists of a bare quark–gluon core and a pion cloud, and the large pion cloud contribution to CMR can be seen by comparing the Sato–Lee solid and dashed curves in Fig. 3. We further observe that the dashed curve of the Sato–Lee "bare" component is qualitatively similar to the prediction of a model based on the Dyson–Schwinger Equation of QCD [59] (DSEM). Since DSEM does not include the pion degree of freedom, the agreement between the data and the Sato–Lee prediction sug-

gests a possible link between the bare quark-core of a dynamical model and the genuine QCD dynamics.

The new data have accessed a kinematic region where, for the first time, a more drastic change of the CMR magnitude with Q^2 is observed compared to the trend of the world data in the region higher than $Q^2 = 0.1$ (GeV/c)^2. The results suggest that the values of the CMR and EMR ratios converge as $Q^2 \to 0$. This is well described by the Sato–Lee model, and considering that the bare CMR and EMR values of the model are equal at $Q^2 = 0$ due to the use of the long-wave limit, the convergence of the CMR and EMR ratios at $Q^2 = 0$ suggests that the meson cloud contribution to both quadrupole amplitudes is similar as we enter the low Q^2 regime.

In Fig. 3 one can also identify the success of the large-Nc calculation [58] in the prediction of the CMR ratio. Nevertheless the calculation underestimates the values the magnetic dipole and of the quadrupole amplitudes by $\approx 20\%$ but this effect cancels out in the ratio. Constituent quark model (CQM) predictions are known to considerably deviate from the experimental results. Two representative CQM calculations are shown in Fig. 3, that of Capstick [9] and of the hypercentral quark model (HQM) [50], which fail to describe the data. It demonstrates that the color hyperfine interaction is inadequate to explain the effect at large distances. Chiral
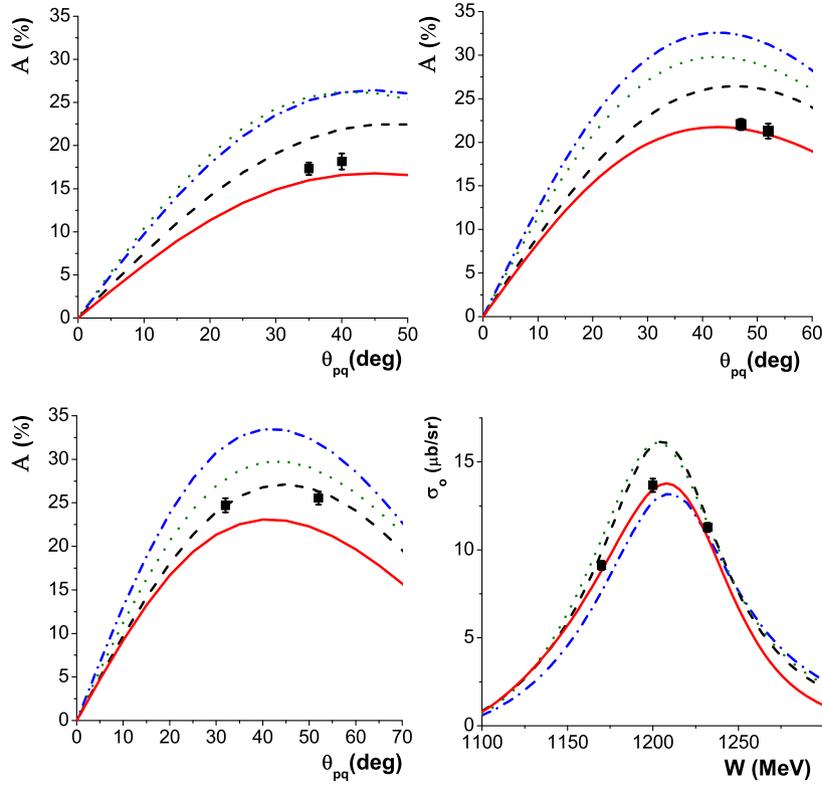
Fig. 2. Top panels: asymmetries at $Q^2 = 0.04$ (GeV/c)^2 (left) and $Q^2 = 0.09$ (GeV/c)^2 (right). Bottom panels: asymmetries (left) and σ_0 (right) at $Q^2 = 0.13$ (GeV/c)^2. The definition of the theoretical curves is given at the caption of Fig. 1.
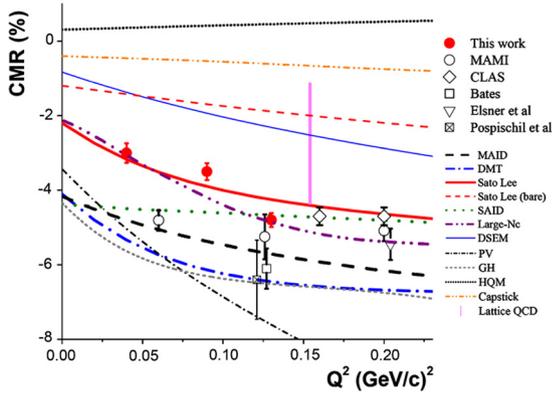

Fig. 3. The CMR measurements as a function of Q^2. The results from this work (solid circles) and from [14,23,25,37,38,40] (open symbols) are presented. All data points are shown with their total experimental uncertainties (statistical and systematic) added in quadrature. The theoretical predictions of MAID [33,34], DMT [32], SAID [36], Sato-Lee [31], Capstick [9], HQM [50], the Lattice-QCD calculation [28], the large-Nc calculation [58], the DSEM [59], the ChEFT of Pascalutsa–Vanderhaegen (PV) [48] and the Gail–Hemmert (GH) [49] are also shown.

effective field theoretical calculations [48,49] also account for the magnitude of the effects giving further credence to the dominance of the meson cloud at the low momentum transfer region. Chiral perturbation theory offers the natural framework to investigate the role of pionic contributions to the nucleon structure where nucleon observables receive contribution from pion loops, the "pion cloud", but it has to be noted that such contributions are in general not scale-independent [60] and thus can not provide a model independent definition.

Lattice QCD results [28] allow a comparison to experiment with the chirally extrapolated [48] values of CMR found to be nonzero and negative in the low Q^2 region. Lattice QCD calculations [61] that utilize improved methods are currently ongoing and will provide results at lower Q^2, with reduced uncertainties, and with lighter quark masses of 180 MeV. These calculations so far indicate [61] that the discrepancy between Lattice QCD and the data gets smaller as the pion mass approaches the physical value. Lattice QCD calculations with pion mass close to the physical are now within reach in the near future. The new results provided by this experiment offer important, high precision, benchmark quantities. Namely, at physical value of the pion mass and after taking the continuum limit Lattice QCD should reproduce the data, otherwise it cannot claim to predict other quantities.

In conclusion, we have reported on new p$(e, e'p)\pi^\circ$ measurements at the $\Delta^+(1232)$ resonance at the low momentum transfer region where the mesonic cloud dynamics are predicted to be dominant and appreciably changing with Q^2. The Coulomb quadrupole amplitude measurements have been extended to a new lowest momentum transfer, and a rapid fall-off of the magnitude of the CMR ratio below $Q^2 = 0.1$ (GeV/c)^2 has been observed for the first time at low Q^2. The reported measurements reveal, for the first time, that the values of the two quadrupole amplitudes converge as $Q^2 \to 0$. The measured resonant amplitudes are in disagreement with the values predicted by quark models on account of the noncentral color-hyperfine interaction. On the other hand, the dominant role of the mesonic degrees of freedom has been demonstrated at the large distance scale. The new data are described with a remarkable success from a dynamical model that suggests that more than half of the magnitude of the Coulomb quadrupole amplitude is attributed to the mesonic cloud at low Q^2. The same conclusion is being further supported by a Dyson–Schwinger calculation Equation Model where the pion degrees of freedom are not included, and the fact that it underestimates the data is a clear and important indication of the dressed-quark component. The results are in qualitative agreement with chiral perturbation theory calculations, and they also provide

important benchmark quantities for the Lattice QCD calculations. Strong experimental constraints have been provided to the theoretical calculations, thus offering the necessary input that will allow their refinement and will resolve the theoretical discrepancies.

References

[1] A.M. Bernstein, Eur. Phys. J. A 17 (2003) 349.
[2] Jefferson Lab proposal PR12-15-001.
[3] H. Fonvieille, et al., Phys. Rev. C 86 (2012) 015210.
[4] N. Sparveris, et al., Study of the nucleon structure by Virtual Compton Scattering measurements at the Δ resonance, MAMI experiment A1/3-12.
[5] A.M. Bernstein, C.N. Papanicolas, AIP Conf. Proc. 904 (2007) 1.
[6] A. de Rujula, H. Georgi, S.L. Glashow, et al., Phys. Rev. D 12 (1975) 147.
[7] S.L. Glashow, Physica 96A (1979) 27.
[8] N. Isgur, G. Karl, R. Koniuk, Phys. Rev. D 25 (1982) 2394.
[9] S. Capstick, G. Karl, Phys. Rev. D 41 (1990) 2767.
[10] G. Blanpied, et al., Phys. Rev. Lett. 79 (1997) 4337.
[11] R. Beck, et al., Phys. Rev. Lett. 78 (1997) 606;
     R. Beck, et al., Phys. Rev. Lett. 79 (1997) 4515 (Erratum).
[12] R. Beck, et al., Phys. Rev. C 61 (2000) 035204.
[13] V.V. Frolov, et al., Phys. Rev. Lett. 82 (1999) 45.
[14] T. Pospischil, et al., Phys. Rev. Lett. 86 (2001) 2959.
[15] C. Mertz, et al., Phys. Rev. Lett. 86 (2001) 2963.
[16] P. Bartsch, et al., Phys. Rev. Lett. 88 (2002) 142001.
[17] L.D. van Buuren, et al., Phys. Rev. Lett. 89 (2002) 012001.
[18] K. Joo, et al., Phys. Rev. Lett. 88 (2002) 122001.
[19] N.F. Sparveris, et al., Phys. Rev. C 67 (2003) 058201.
[20] C. Kunz, et al., Phys. Lett. B 564 (2003) 21.
[21] K. Joo, et al., Phys. Rev. C 68 (2003) 032201.
[22] K. Joo, et al., Phys. Rev. C 70 (2004) 042201.
[23] N.F. Sparveris, et al., Phys. Rev. Lett. 94 (2005) 022003.
[24] J.J. Kelly, et al., Phys. Rev. Lett. 95 (2005) 102001.
[25] S. Stave, et al., Eur. Phys. J. A 30 (2006) 471.
[26] M. Ungaro, et al., Phys. Rev. Lett. 97 (2006) 112003.
[27] Z.L. Zhou, et al., Nucl. Instrum. Methods A 487 (2002) 365.
[28] C. Alexandrou, et al., Phys. Rev. Lett. 94 (2005) 021601.
[29] C. Alexandrou, et al., Phys. Rev. D 77 (2008) 085012.
[30] C. Alexandrou, et al., Phys. Rev. D 83 (2011) 014501.
[31] T. Sato, T.-S.H. Lee, Phys. Rev. C 63 (2001) 055201.
[32] S.S. Kamalov, S.N. Yang, Phys. Rev. Lett. 83 (1999) 4494.
[33] S.S. Kamalov, et al., Phys. Lett. B 522 (2001) 27.
[34] D. Drechsel, et al., Nucl. Phys. A 645 (1999) 145.
[35] D. Drechsel, L. Tiator, J. Phys. G 18 (1992) 449.
[36] R.A. Arndt, et al., Phys. Rev. C 66 (2002) 055213, arXiv:nucl-th/0301068, http://gwdac.phys.gwu.edu.
[37] D. Elsner, et al., Eur. Phys. J. A 27 (2006) 91–97.
[38] N.F. Sparveris, et al., Phys. Lett. B 651 (2007) 102.
[39] S. Stave, et al., Phys. Rev. C 78 (2008) 025209.
[40] I.G. Aznauryan, et al., Phys. Rev. C 80 (2009) 055203.
[41] A.N. Villano, et al., Phys. Rev. C 80 (2009) 035203.
[42] J. Kirkpatrick, et al., Phys. Rev. C 84 (2011) 028201.
[43] N. Sparveris, et al., Eur. Phys. J. A 49 (2013) 136.
[44] N. Sparveris, et al., Phys. Rev. C 78 (2008) 018201.
[45] D.-H. Lu, A.W. Thomas, A.G. Williams, Phys. Rev. C 55 (1997) 3108.
[46] U. Meyer, E. Hernandez, A.J. Buchmann, Phys. Rev. C 64 (2001) 035203.
[47] M. Fiolhais, B. Golli, S. Sirca, Phys. Lett. B 373 (1996) 229.
[48] V. Pascalutsa, M. Vanderhaeghen, Phys. Rev. D 73 (2006) 034003.
[49] T.A. Gail, T.R. Hemmert, Eur. Phys. J. A 28 (1) (2006) 91–105.
[50] M. De Sanctis, et al., Nucl. Phys. A 755 (2005) 294.
[51] J. Mandeville, et al., Phys. Rev. Lett. 72 (1994) 3325–3328.
[52] B. Pasquini, M. Gorchtein, D. Drechsel, A. Metz, M. Vanderhaeghen, Eur. Phys. J. A 11 (2001) 185–208.
[53] D. Drechsel, B. Pasquini, M. Vanderhaeghen, Phys. Rep. 378 (2003) 99–205.
[54] J. Alcorn, et al., Nucl. Instrum. Methods A 522 (2004) 294.
[55] MCEEP, Monte Carlo for (e,e'p) experiments, http://hallaweb.jlab.org/software/mceep/mceep.html.
[56] D. Anez, Ph.D. thesis, Dalhousie University, 2014.
[57] A. Blomberg, Ph.D. thesis (in preparation), Temple University, 2015.
[58] V. Pascalutsa, M. Vanderhaeghen, Phys. Rev. D 76 (2007) 111501.
[59] Jorge Segovia, Ian C. Cloët, Craig D. Roberts, Sebastian M. Schmidt, Few-Body Syst. 55 (2014) 1185–1222.
[60] U. Meissner, AIP Conf. Proc. 904 (2007) 142–150, arXiv:nucl-th/0701094.
[61] C. Alexandrou, private communication, submitted for publication.